APPLICATION

Multi-objective process parameter optimization for minimizing weldline and cycle time using heater-assisted rapid heat cycle molding

Satoshi Kitayama[1] · Shogo Tsurita[2] · Masahiro Takano[3] · Yusuke Yamazaki[4] · Yoshikazu Kubo[4] · Shuji Aiba[4]

Abstract

Rapid heat cycle molding (RHCM) that actively controls the mold temperature is an innovative plastic injection molding (PIM) technology. The melt plastic smoothly flows into cavity due to the high mold temperature, and weldline reduction can be achieved. The overall mold heating in the conventional RHCM leads to long cooling time, which makes the cycle time long. To shorten the cycle time as well as weldline reduction, the RHCM using a heater called the heater-assisted RHCM is developed. It is easy to install the heater in the mold, and the local region around which the weldline is observed is heated up. Consequently, the weldline will be reduced. Since the mold is locally heated up, short cycle time will be expected. Since the process parameters in the heater-assisted RHCM are unknown in advance, design optimization is used to determine the process parameters. The numerical simulation is computationally so expensive that sequential approximate optimization that response surface is repeatedly constructed and optimized is adopted to determine the optimal process parameters. It is found from the numerical result that the weldline and the cycle time are well reduced. Based on the numerical result, the experiment using the PIM machine (MS100, Sodick) is conducted. It is confirmed through the numerical and experimental result that the heater-assisted RHCM is effective to the weldline reduction and the short cycle time.

Keywords Plastic injection molding · Heater-assisted rapid heat cycle molding · Multi-objective optimization, Numerical simulation · Sequential approximate optimization

✉ Satoshi Kitayama
  kitayama-s@se.kanazawa-u.ac.jp

  Shogo Tsurita
  stsurita@stu.kanazawa-u.ac.jp

  Masahiro Takano
  takano@irii.jp

  Yusuke Yamazaki
  yamazaki-y@sodick.co.jp

  Yoshikazu Kubo
  kuboy@sodick.co.jp

  Shuji Aiba
  aibas@sodick.co.jp

1 Kanazawa University, Kakuma-Machi, Kanazawa 920-1192, Japan

2 Graduate School of Natural Science & Technology, Kanazawa University, Kakuma-Machi, Kanazawa 920-1192, Japan

3 Industrial Research Institute of Ishikawa, 2-1, Kuratsuki, Kanazawa 920-8203, Japan

4 Sodick Co., Ltd, Ka-1-1, Miya-Machi, Kaga-Shi, Ishikawa 922-0595, Japan

1 Introduction

Many plastic products are produced by plastic injection molding (PIM) and have several advantages such as lightweight, high gloss appearance, high anticorrosion, and high productivity. Conventional PIM process mainly consists of (1) filling phase that melt plastic is injected into the cavity, (2) packing phase that the melt plastic is packed with packing pressure, and (3) cooling phase that the melt plastic is cooled down for the solidification. In the above phases, the melt temperature, the injection time, the packing pressure, the packing time, the cooling time, and the cooling temperature are the major process parameters, and warpage, volume shrinkage, sink mark, and weldlines are the major defects in the PIM. For high product quality, the process parameters are conventionally adjusted through the trial-and-error method. Among the defects, weldlines that are formed when two or more melt fronts meet affect not only the strength but also the surface appearance of a product, and it is important to reduce the weldlines as much as possible for high surface quality. The process parameter

optimization is valid to the weldline reduction [1], and several papers have been published.

Li et al. investigated the effect of process parameters on weldline by using the Taguchi method [2], in which they clarified that high melt temperature and high injection speed led to the weldline reduction. Wu and Liang also investigated the effect of process parameters on the weldline using the Taguchi method [3], from which it was clarified that the melt temperature, the mold temperature, the injection velocity, and the packing pressure were influential to the weldline strength. Ozcelik optimized the process parameters (the melt temperature, the packing pressure, and injection pressure) for high mechanical properties by the Taguchi method [4]. Kim et al. also optimized both the process parameters (the injection time, the melt temperature, and the mold temperature) and the gate locations for the weldline reduction of an automobile front bumper using Taguchi method [5]. Deng et al. optimized several process parameters (mold temperature, melt temperature, and injection time) for minimizing warpage, weldline, and air trap of a power outlet plastic product [6], in which multi-objective particle swarm optimization (MOPSO) was adopted to identify the Pareto frontier. Note that this paper directly optimizes the process parameters without using the response surface. Kitayama performed the process parameter optimization for minimizing weldline and clamping force [7], in which it was reported that the trade-off between the weldline and the clamping force was clarified and high clamping force led to the weldline reduction. Unlike Refs. [2, 4, 5], sequential approximate optimization (SAO) that response surface was repeatedly constructed and optimized was adopted for the design optimization. Feng and Zhou determined the optimal process parameters for minimizing the warpage, the shrinkage, and the weldline of an air-conditioner vent [8], in which radial basis function was adopted for constructing the response surface of each objective function and the multi-objective genetic algorithm (MOGA) was used to identify the Pareto frontier. Zhou et al. optimized the process parameters in PIM for minimizing four objectives (the warpage, the weldline, the clamping force, and the cycle time) [9], in which the quadratic polynomial approximation was adopted for the response surface. In this paper, the sensitivity information at the sampling points was considered for highly accurate response surface. These papers perform the process parameter optimization for weldline reduction using the conventional PIM consisting of the filling, packing, and cooling phase. However, it has been well recognized that rapid heat cycle molding (RHCM) that actively controls the mold temperature is more effective to weldline reduction [10].

The concept of RHCM is explained using Fig. 1, in which the mold temperature profile is shown with the solid line, and t_h, t_{inj}, t_p, and t_c represent the heating time, the injection time, the packing time, and the cooling time, respectively.
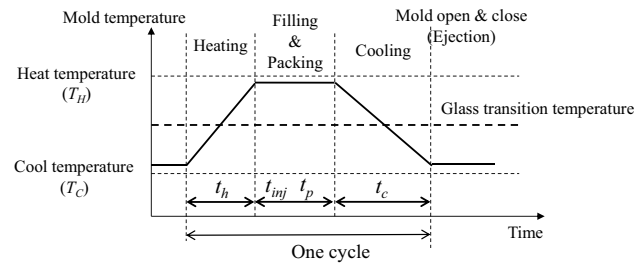
Fig. 1 Typical mold temperature profile of RHCM

Unlike the conventional PIM, the mold is rapidly heated above the glass transition temperature of a material before the filling phase (this phase is called the heating phase), and then, the melt plastic is injected into the cavity. After the packing phase, the mold is cooled down for the solidification. The melt plastic smoothly flows into the cavity due to the high mold temperature, and the weldline will be reduced.

Chen et al. adopted an electromagnetic induction heating for the RHCM and investigated the effect on weldline reduction [11], from which it was found that the mold surface was uniformly heated by the induction heating and the weldline could successfully be reduced. Chang and Hwang developed an infrared rapid surface heating system [12]. The mold surface temperature could rise from 83 °C to 188 °C with 15 s, and the filling ability enhanced. Li et al. optimized the layout of heating/cooling channels of a steam-assisted RHCM [13], in which the distribution of mold temperature was minimized for uniformity and the experiment for a LCD TV panel was also conducted. It was found from the experiment that high surface quality product could be obtained, but the weldline and the cycle time were not discussed. Electric-assisted RHCM was conducted by Zhao et al. [14], in which the mold was heated through the heating rod and was cooled down with the cooling channel. It was reported that the cycle time of electric-assisted was almost the same as that of conventional PIM. The authors also compared the steam- and the electric-assisted RHCM [15], from which it was found that the latter could improve the heating speed with large energy consumption and the cooling efficiency could also be enhanced, compared with the steam-assisted RHCM. The layout optimization of heating/cooling channels for minimizing the distribution of mold temperature and the heating time in steam- and electric-assisted RHCM was performed [16, 17], from which it was found that the heating/cooling channels played an important role for the short heating time as well as the temperature distribution uniformity. These papers mainly discuss the distribution of mold temperature or the layout of heating/cooling channels, and the effect of RHCM on the surface appearance and weldline is not discussed. Wang et al. investigated the effect of mold temperature on the weldline using an electric-assisted RHCM [18], in which

it was clarified that the high mold temperature during the filling phase was effective to the weldline reduction and the weldline was completely eliminated by the proposed RHCM unlike the conventional PIM. However, the effect of other process parameters such as the melt temperature, the injection time, the packing pressure, and the packing time on the weldline reduction was not discussed. Wang et al. developed a water-assisted RHCM that water was used to control the mold temperature [19]. The layout of heating/cooling channels was determined so as to minimize both the heating time and the distribution of mold temperature, and the high-gloss and weldless panel product was obtained. However, the process parameters were not discussed. The layout optimization of the heating rod for an electric-assisted RHCM was performed by Xiao and Huang [20, 21], in which the heating time and the distribution of mold temperature were minimized like Ref. [19]. Other applications using steam- and electric-assisted RHCM can be found in Refs. [22, 23], but these are mainly focused on the cooling channel design. Unlike the above papers, Kitayama et al. performed the process parameter optimization using a water-assisted RHCM [24], in which the mold temperature was maximized for the weldline reduction whereas the cycle time was minimized for the high productivity. The water-assisted RHCM successfully reduced the weldline, but required long heating/cooling time. As the result, the productivity was low in comparison with the conventional PIM. The temperature controllers to control the coolant temperature were also required, and the system was expensive. Kirchheim et al. developed a conformal cooling channel using additive manufacturing based on laser powder bed fusion and investigated the temperature distribution of a product [25], in which the mold was heated and cooled like the RHCM. It was found from the numerical result that the temperature was more uniformly distributed by the cooling channel and the cooling time was well reduced. However, the mold temperature profile was determined by the engineer's experience. Xiao et al. developed an RHCM using electric heating and investigated the effect on the surface appearance of a product [26, 27], from which it was found that high mold temperature improved the surface quality. Wang et al. investigated the effect on the mechanical strength of weldline with and without RHCM using electric heating [28], in which the mold temperature before the filling phase (heat temperature in Fig. 1) was discussed. It was reported that the tensile strength increased as the mold temperature rose. Unfortunately, the mold temperature profile in Fig. 1 and the cycle time were not well discussed in these papers [26–28].

The representative papers on the RHCM are listed in Table 1, from which the process parameter optimization is rarely discussed in the literature. This implies that the process parameters in RHCM are completely determined by engineer's experience. In addition, many papers mainly focus on the layout of heating/cooling channels so as to minimize the temperature distribution or the heating time. In particular, the temperature distribution uniformity leads to not only high gloss appearance, but also warpage reduction [29]. However, the conventional RHCM heats the mold globally, and long cooling time is required. Consequently, the cycle time is long. To shorten the cooling time, it is effective to heat the mold locally. In the case of weldline reduction, it will be effective to heat the local region around which the weldline is observed. The local heating has already been proposed by Nian et al. [30], in which the cooling channels were designed based on the neutral axis theory. Therefore, the cooling

Table 1 Representative papers on RHCM

Authors	Year	Ref	RHCM	Process parameter optimization	Objective function(s)
Chen et al	2006	7	Induction heating	Not performed	N/A
Chang and Hwang	2006	8	Infrared	Not performed	N/A
Li et al	2009	9	Steam-assisted	Not performed	Mold temperature distribution is minimized
Zhao et al	2011	10	Electric-assisted	Not performed	N/A
Wang et al	2011	12	Steam-assisted	Not performed	N/A
Wang et al	2011	13	Electric-assisted	Not performed	Heating time is minimized Mold temperature distribution is minimized
Wang et al	2013	15	Water-assisted	Not performed	Heating time is minimized Mold temperature distribution is minimized
Xiao and Huang	2014	16, 17	Electric-assisted	Not performed	Heating time is minimized Mold temperature distribution is minimized
Wang et al	2014	18	Steam-assisted	Not performed	N/A
Wang et al	2018	19	Electric-assisted	Not performed	N/A
Kitayama et al	2019	20	Water-assisted	Performed	Mold temperature is maximized Cycle time is minimized

channels with the product shape were designed, and different temperature to each cooling channel was set. As the result, it was reported that warpage of a portable cover was well reduced. The idea of local heating is applicable to the weldline reduction using the RHCM, but it is also necessary to consider the cycle time for high productivity. In other words, the process parameter optimization in RHCM considering the product quality and productivity should be performed.

Here, the objective of this paper is summarized as follows.

1. Heater-assisted RHCM that a heater is installed in the mold is proposed. The heater is installed to a region around which the weldline is observed. The mold is locally heated up for smoothly flowing the melt plastic, and consequently, the weldline will be reduced.
2. The mold is locally heated up, and the cooling time will then be shorter than one using the conventional RHCM that the mold is uniformly heated. As the result, high productivity will be expected.
3. The process parameters in heater-assisted RHCM strongly affect the weldline and the cycle time. High mold temperature is valid to the weldline reduction, whereas long cooling time is generally required. Conventionally, these are determined by engineer's experience. In this paper, design optimization is performed to determine the optimal process parameters. Based on Refs. [2, 3, 5–7], it is considered that the injection time is an effective process parameter for weldline reduction. In addition, considering the characteristics of RHCM, the mold temperature is also an effective process parameter for surface appearance [11, 24, 26]. A novel objective function for weldline reduction considering both process parameters is proposed in this paper.
4. As Shayfull et al. suggested in Ref. [31], the conformal cooling channels can heat and cool the mold uniformly, and it is desirable to use it for the heater-assisted RHCM. Recently, it is possible to fabricate the conformal cooling channels by using metal 3D printer, and the confor-

mal cooling channels attract attention [32–34]. Then, the conformal cooling channel is used in this paper.
5. The experiment using the heater-assisted RHCM is conducted to examine the validity. The PIM machine (MS100, Sodick) is used in the experiment.

The rest of this paper is organized as follows. The target product and the numerical simulation model are shown in Sect. 2. Section 3 describes the design optimization problem for the weldline reduction and the short cycle time using the heater-assisted RHCM. The numerical and experimental result is shown in Sect. 4. Finally, the experimental result using PIM machine (MS100, Sodick) is presented.

2 Target product and numerical simulation using heater-assisted rapid heat cycle molding

The target product and the numerical simulation model are shown in Figs. 2 and 3, respectively. Moldex3D (2021R3) is used for the numerical simulation. As show in Fig. 3, the heater is installed in the mold, and the conformal cooling channel is used to uniformly cool down the mold. The flow process without the heater is shown in Fig. 4, in which the initial process parameters listed in Table 2 are used. It is found that the thickness of side wall is different and then the weldline is observed around the center of side wall. The weldline length is 7.1 mm when the conventional PIM (without using the heater) using the initial process parameters is performed. Then, as shown in Fig. 3, the heater is installed around which the weldline is observed. The polyacetal resin is used as the material, and the material property is listed in Table 3.

The numerical simulation of heater-assisted RHCM is carried out as follows. First, the mold is heated above the glass transition temperature of the material using the heater in the heating phase, and the heating time (t_h in Fig. 1) is the major process parameter. Note that the heat temperature
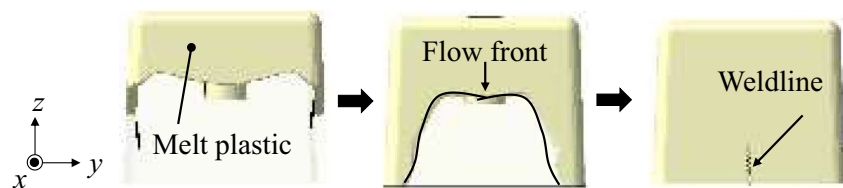
Fig. 2 Target product

Unit [mm]
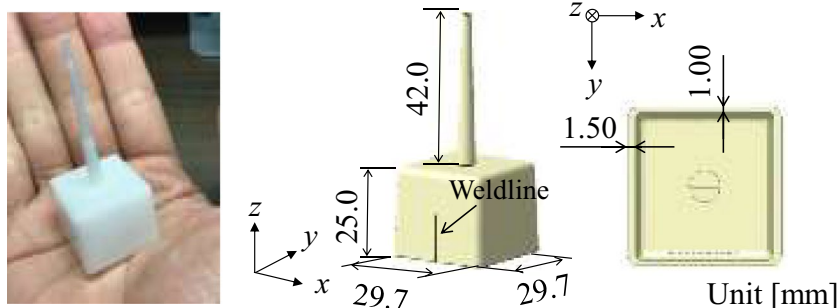
Fig. 3 Conformal cooling channel and heater
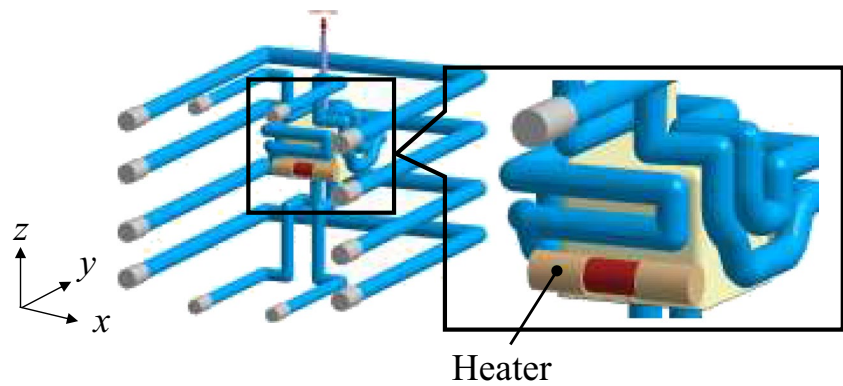
Heater

Fig. 4 Flow process and weldline

Flow front

Melt plastic
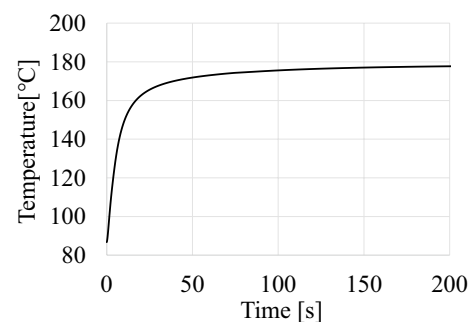
Weldline

Table 2 Initial process parameters without heating

Melt temperature (°C)	Injection time (s)	Packing pressure (MPa)	Packing time (s)	Cooling temperature (°C)	Cooling time (s)
190	3.0	50	5	70	20

Table 3 Material property of polyacetal resin

Melt density (g/cm^3)	1.19
Eject temperature (°C)	135
Elastic module (GPa)	2.8
Poisson ratio	0.38
Specific heat (J/(kg·°C))	2503
Melting temperature (°C)	155
Material characteristics	Crystalline
Recommended mold temperature (°C)	60–80
Recommended melt temperature (°C)	180–210

Fig. 5 Performance of heater

in Fig. 1 completely depends on the performance of heater and the performance in this paper is shown in Fig. 5, from which it is found that the longer the heating time is, the higher the mold temperature is. It is possible to rise the mold temperature from 86 °C to 150 °C with 10 s.

The melt plastic is injected into the cavity after the heating phase, and the melt plastic is finally cooled down for the solidification. The process of heater-assisted RHCM is so simple, but the heating time strongly affects the surface appearance of the product. The flow of melt plastic and the weldline is shown in Fig. 6, in which the temperature distribution at the end of heating phase is shown in this figure.

As shown in Fig. 6a, the weldline is long due to the low mold temperature when the heating time is short. On the other hand, high temperature makes the weldline short, but the burn will often be observed on the surface in the experiment (unfortunately, it is difficult to simulate the burn in the current numerical simulation). It is also found from Fig. 6 that the flow of melt plastic is completely different due to the local heating. It is reported that the flow of melt plastic is so closely related to the weldline [35], and it is expected that the weldline will be reduced by introducing the local heating.
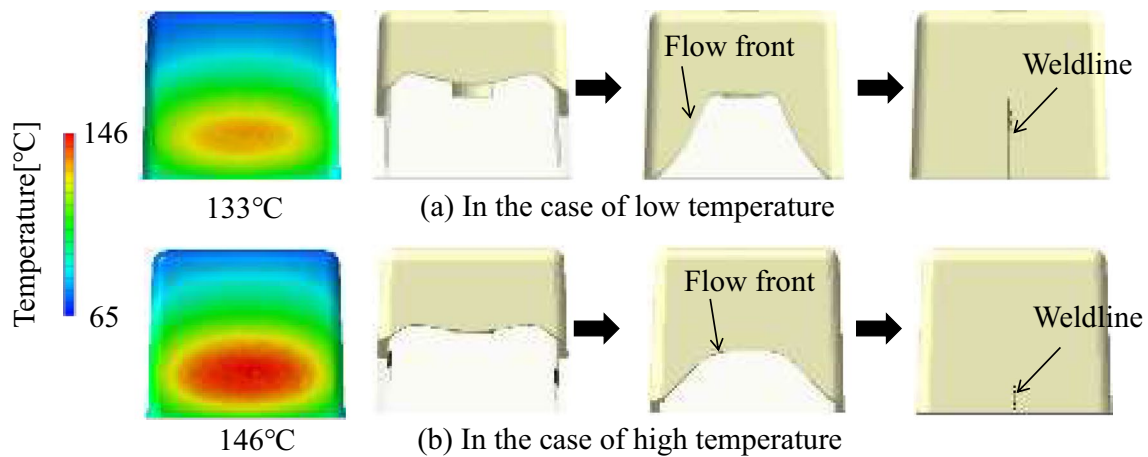
Fig. 6 Flow of melt plastic and weldline

3 Process parameter optimization in heater-assisted rapid heat cycle molding

3.1 Multi-objective optimization

Multi-objective optimization problem is generally formulated as follows.

$$\left.\begin{array}{l} (f_1(x), f_2(x), \cdots, f_K(x)) \to min \\ x_i^L \le x_i \le x_i^U \quad i = 1, 2, \cdots, n \\ g_k(x) \le 0 \quad k = 1, 2, \cdots, ncon \end{array}\right\} \quad (1)$$

where $f_i(\boldsymbol{x})$ is the i-th objective function to be minimized and K represents the number of objective functions. $x = (x_1, x_2, \cdots, x_n)^T$ denotes the design variables, x_i denotes the i-th design variable, and n represents the number of design variables. x_i^L and x_i^U are the lower and upper bounds of the i-th design variable. $g_k(\boldsymbol{x})$ denotes the k-th design constraint, and $ncon$ represents the number of design constraints. To determine the process parameters (design variables), a multi-objective optimization is solved. Therefore, a set of Pareto optimal solutions is identified.

3.2 Process parameters (design variables)

The process parameters in heater-assisted RHCM are summarized as follows.

In heating phase: the heating time (t_h).

In the filling and packing phase: the melt temperature (T_{melt}), the injection time (t_{inj}), the packing pressure (p), and the packing time (t_p).

In the cooling phase: the cooling temperature (T_C) and the cooling time (t_c).

Therefore, the process parameters $\boldsymbol{x}$ is given as $x = (t_h, T_{melt}, t_{inj}, p, t_p, T_c, t_c)^T$, and the range of the process parameters is defined by Eq. (2).

$$\left.\begin{array}{l} 5 \le t_h \le 30[s] \quad 180 \le T_{melt} \le 210[°C] \quad 0.5 \le t_{inj} \le 3.0[s] \\ 10 \le p \le 70[MPa] \quad 1 \le t_p \le 10[s] \quad 60 \le T_c \le 80[°C] \\ 1 \le t_c \le 30[s] \end{array}\right\} \quad (2)$$

The range of process parameters is determined for the following reasons.

(1) The heating time (t_h): the upper bound is determined by considering the performance of heater (see Fig. 5).
(2) The melt temperature (T_{melt}) and the cooling temperature (T_c): the recommended value of Moldex3D is directly used.
(3) The injection time (t_{inj}): referring to Table 2, the upper bound is set to 3.0 s.
(4) The packing pressure (p): the mold will be damaged over 70 MPa, and the upper bound is set to 70 MPa.
(5) The packing time (t_p): considering the gate seal time, the upper bound is set to 10 s.
(6) The cooling time (t_c): considering the performance of heater and the recommended value of Moldex3D, the upper bound is set to 30 s.

3.3 Objective functions

To reduce the weldline using the heater-assisted RHCM, the mold temperature (T_{mold}) is maximized [24]. The illustrative example is shown in Fig. 7, from which it is clear that the higher the mold temperature is, the shorter the weldline is. It is also reported that the short injection time leads to the weldline reduction [2, 5, 36]. It is preferable to consider the effect of
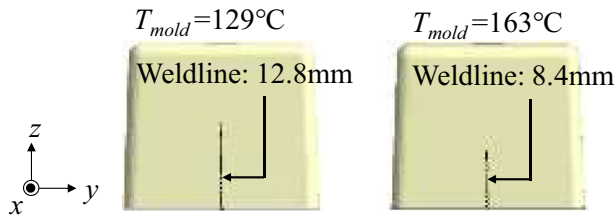
Fig. 7 Weldline with different mold temperatures

Fig. 8 Short shot (left hand: numerical simulation, right hand: experiment)

the mold temperature and the injection time on the weldline reduction, and then, the ratio between the mold temperature and the injection time is maximized [37]. Therefore, the first objective function is given by Eq. (3).

$$f_1(x) = \frac{T_{mold}}{t_{inj}} \rightarrow max \tag{3}$$

For high mold temperature, long heating time is required in the heater-assisted RHCM. Many papers consider the heating time as listed in Table 1, and it is important to minimize the heating time for high productivity. However, short heating time makes the mold temperature low. As shown in Fig. 6, the low mold temperature results in the long weldline. To consider the productivity, the cycle time should be taken into account. Then, the cycle time is taken as the second objective function to be minimized, which is given by the explicit form of the design variables as shown in Eq. (4).

$$f_2(x) = t_h + t_{inj} + t_p + t_c \rightarrow min \tag{4}$$

3.4 Design constraint (short shot)

The target product has different thickness, and the flow of melt plastic in the side wall is also different. Inappropriate process parameters easily lead to short shot that the melt plastic is not filled into the cavity. The illustrative example of short shot in the numerical simulation and the experiment is shown in Fig. 8. The short shot should strongly be avoided in the PIM and is handled as the design constraint.

To evaluate the short shot, the following equation is used [7].

$$V_s = 1 - \frac{V}{V_0} \tag{5}$$

where V and V_0 represent the melt plastic volume and the cavity volume, respectively. The positive value of Eq. (5) indicates the short shot. The design constraint $g_1(x)$ is then evaluated as follows:

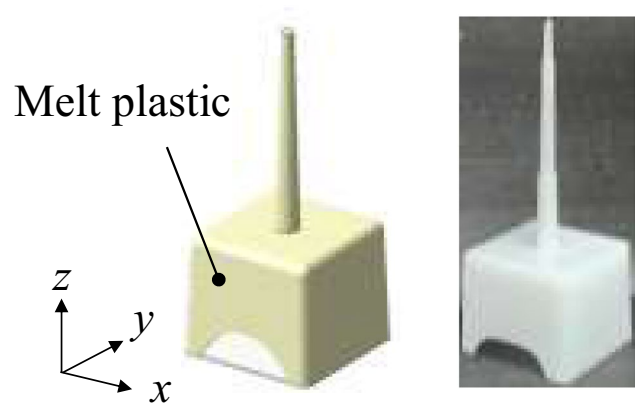$$g_1(x) = \begin{cases} V_s & V_s > 0 \\ 0 & \text{otherwise} \end{cases} \tag{6}$$

3.5 Sequential approximate optimization

To identify the Pareto frontier between mold temperature and cycle time, the SAO using radial basis function (RBF) network in Ref. [38] is used. By using this system, we have already resolved several engineering issues such as sheet metal forming using servo press [39–41], process parameter optimization in cold forging [42], and energy management system and optimization for hybrid electric vehicle [43]. Then, this is used as the design optimization tool. See Ref. [44] for the details of RBF network. The numerical procedure is briefly described.

(STEP1) The Latin hypercube design (LHD) is used to generate several sampling points (the combination of process parameters).

(STEP2) The numerical simulation for heater-assisted RHCM is conducted at the sampling points. Through the numerical simulation, the objective functions (Eqs. (3) and (4)) and the design constraint (Eq. (6)) are numerically evaluated.

(STEP3) The response surface using the RBF network is constructed. Here, the response surface of objective functions and design constraint is described as $\widetilde{f}_1(x)$, $\widetilde{f}_2(x)$, and $\widetilde{g}_1(x)$.

(STEP4) The weighted lp norm defined by Eq. (7) is used to determine the Pareto optimal solutions.

$$\left. \begin{array}{l} \left[\sum_{k=1}^2 \left(w_k \widetilde{f}_k(x) \right)^p \right]^{1/p} \rightarrow min \\ x_i^L \leq x_i \leq x_i^U \quad i = 1, 2, , n \\ \widetilde{g}_1(x) \leq 0 \end{array} \right\} \tag{7}$$

where w_k ($k = 1, 2$) represents the weight of the k-th objective function and p is the parameter. According to Refs. [39–43], p is set to 4. Various weights are assigned in order to determine a set of Pareto optimal solutions.

(STEP5) If a terminal criterion is satisfied, the SAO algorithm will terminate. Otherwise, the Pareto optimal solutions in

STEP4 are added as the new sampling points for improving the accuracy of Pareto frontier. As the result, the number of sampling points increases. Then, the algorithm returns to STEP2.

As the terminal criterion, the error between the numerical simulation and the response surface at the Pareto optimal solutions is considered. When the error is within 5%, the algorithm terminates. The flow of the SAO algorithm is shown in Fig. 9.

4 Numerical and experimental result

4.1 Numerical result

Twenty initial sampling points are generated by the LHD, and the Pareto frontier between $f_1(x)$ and $f_2(x)$ is identified. The result is shown in Fig. 10 with the weldline, in which the black circles denote the Pareto optimal solution. Note that the white circle denoted as "conventional PIM" is the result using the process parameters in Table 2. Among the Pareto optimal solutions, two points (A and B) are selected for the comparison, and the optimal process parameters at these points are listed in Table 4.

It is found from Fig. 10 that the weldline can successfully be reduced, compared with the one using the conventional PIM. In particular, there are no weldline at A, and 6.8% improvement of the cycle time can be achieved at B. In Fig. 10, the weldline is observed in the region enclosed by the solid line, whereas no weldline is observed in the region enclosed by the dashed line. It is also found from Fig. 10 that the Pareto frontier is disconnected. The optimal process parameters plotted in Fig. 10 are listed in Table 5. It is found from Table 5 that (1) the smaller t_h is, the shorter the weldline is, (2) T_{melt} is high in the region enclosed by the dashed line, whereas the one in the region
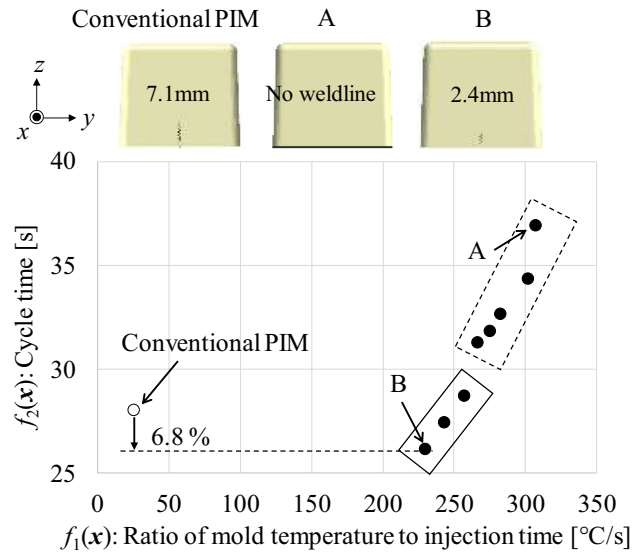

Fig. 10 Pareto frontier between mold temperature and cycle time

enclosed by the solid line is low, (3) t_{inj}, p, and t_p are almost constant in each region but the optimal values exist, and (4) the weldline is eliminated with high T_c. t_c is small in the region enclosed by the dashed line, whereas the one in the region enclosed by the solid line is large. It is difficult to determine the process parameters for weldline reduction in advance, but it is possible to predict the ones for weldline reduction based on Table 5 after the Pareto optimal solutions are determined.

The history of mold temperature at A and B is shown in Fig. 11 with the solid and dashed line, from which it is clear that the longer the heating time is, the higher the mold temperature is. As the result, as shown in Fig. 10, the

Fig. 9 Flow to identify the Pareto frontier using sequential approximate optimization
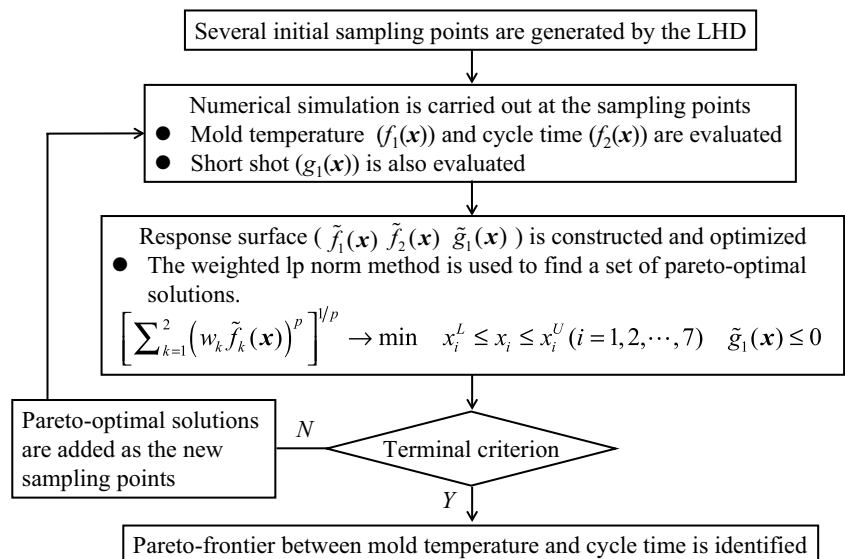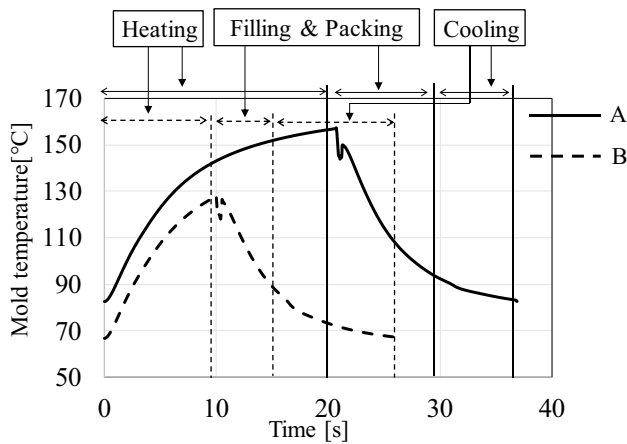
Table 4 Optimal process parameters at A and B

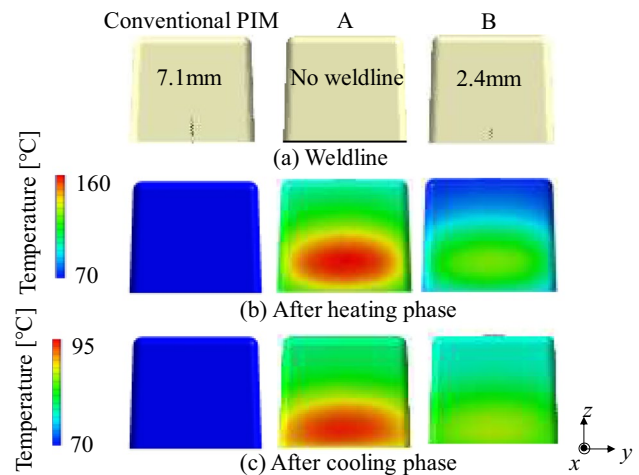|	t_h (s)	T_{melt} (°C)	t_{inj} (s)	p (MPa)	t_p (s)	T_c (°C)	t_c (s)	Cycle time (s)
A	21	205	0.51	12	8.5	76	7	36.9
B	10	193	0.56	29	4.8	62	11	26.1
Conventional PIM	N/A	190	3.00	50	5.0	70	20	28.0

Table 5 Optimal process parameters in Pareto frontier

	t_h (s)	T_{melt} (°C)	t_{inj} (s)	p (MPa)	t_p (s)	T_c (°C)	t_c (s)	
Region enclosed by dashed line	21	205	0.51	12	8.5	76	7	←A
	19	205	0.51	12	8.5	74	6	
	18	205	0.54	12	8.4	73	5	
	18	205	0.55	12	8.4	73	5	
	18	205	0.57	12	8.4	72	5	
Region enclosed by solid line	12	194	0.52	28	5.2	63	11	
	11	193	0.54	28	5.0	62	11	
	10	193	0.56	29	4.8	62	11	←B

Fig. 11 History of mold temperature at A and B

(a) Weldline

(b) After heating phase

(c) After cooling phase

Fig. 12 Comparison of temperature distribution

weldline at A is completely eliminated. The temperature distribution is also shown in Fig. 12. The temperature distribution at A is higher than that at B, and consequently, the weldline is eliminated. However, long cycle time is required for cooling down the mold. The temperature distribution at B after the cooling phase is more uniform than that at A, and this result indicates that the conformal cooling channel is effective to uniformly cooling down the mold. On the other hand, the temperature distribution at A is not uniform due to the high temperature around the weldline. The heating time at A is 21 s, and the maximum mold temperature at the heating phase is approximately 160 °C. Under this condition, it is difficult to uniformly cool down the mold using the conformal cooling channel.

Next, the cycle time listed in Table 4 is compared. As pointed out in Refs. [10, 45], long cycle time is generally required in the RHCM compared with the conventional PIM, but the cycle time at B is improved. The heating time and the cooling time mainly affect the cycle time. The sum of heating and cooling time at B is 21 s, whereas the cooling time of 20 s is required in the conventional PIM. This result shows that the heater-assisted RHCM is effective PIM technology for the weldline reduction without increasing the cycle time.

Finally, the flow of melt plastic is shown in Fig. 13. Compared with the flow of conventional PIM, the one of the heater-assisted RHCM is completely different. In the case of Fig. 13a, c, the separated melt plastic flows denoted by
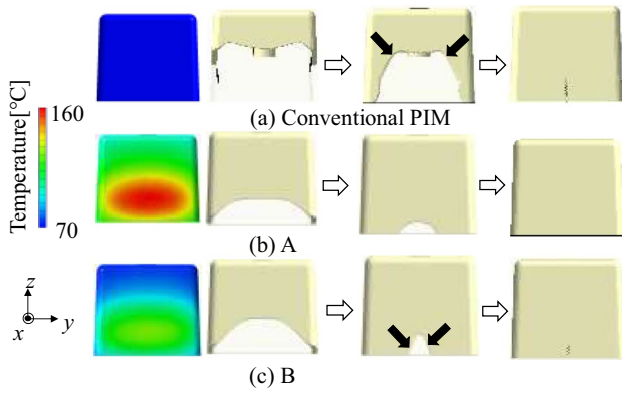
Fig. 13 Flow of melt plastic at A and B

(a) PIM machine (MS100, Sodick)

(b) Die and enlarged view

Fig. 14 PIM machine (MS100, Sodick), die and enlarged view

the black arrow meet around the center of the side wall and the long weldline is formed. On the other hand, as shown in Fig. 13b, the melt plastic is not separated, and consequently, the weldline is not generated. Therefore, the heater-assisted RHCM can vary the flow of melt plastic and the weldline reduction can successfully be achieved.

4.2 Experimental result

The experiment using PIM machine in Fig. 14a (MS100, Sodick) is carried out to examine the validity of heater-assisted RHCM. The die and the enlarged view around the heater are also shown in Fig. 14b. The firerod cartridge heater (Watlow) is used in the experiment and the specification is listed in Table 6. Figure 5 shows the performance of

Table 6 Specification of firerod cartridge heater (Watlow)

Voltage (V)	Capacity (W)	Heat generation density (W/cm^2)	Diameter (mm)
240	225	60.5	6.25

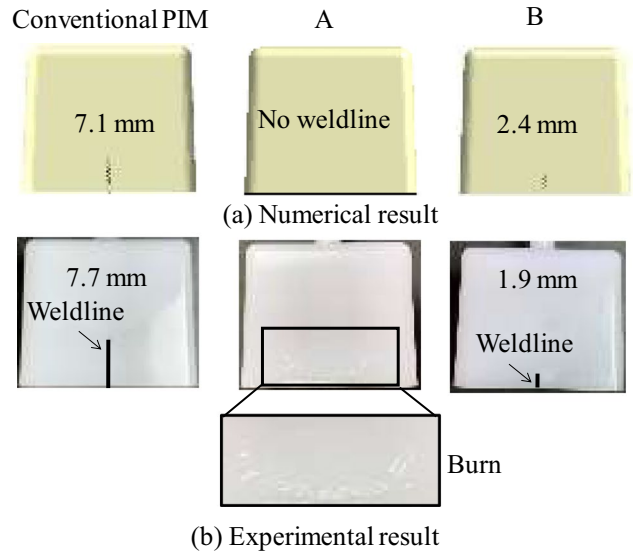
(a) Numerical result

(b) Experimental result

Fig. 15 Experimental results of heater-assisted RHCM

the cartridge heater. The experimental results at three points listed in Table 4 are shown in Fig. 15, in which the black line denotes the weldline. It is found from Fig. 15 that the weldline at B is very short. The weldline at A is completely eliminated but the burn is observed in the experiment. Thus, the weldline is successfully reduced, but it is impossible to avoid the burn in the experiment. As described in Sect. 2, it is difficult to predict the burn in the current numerical simulation. To avoid the burn, the upper bound of heating time should be shortened.

5 Conclusions

The RHCM that actively controls the mold temperature has recently attracted attention for weldline reduction. This paper proposes the heater-assisted RHCM that locally heats the mold for weldline reduction and short cycle time. The heater is installed in the mold, and the RHCM can easily be conducted. However, it is difficult to determine the process parameters. High mold temperature and short injection time can reduce the weldline, and then, the ratio between the mold temperature and the injection time is maximized. On the other hand, the cycle time is minimized for high productivity. Therefore, multi-objective design optimization

is performed to determine the optimal process parameters in the heater-assisted RHCM. The numerical simulation is computationally so expensive that sequential approximate optimization using radial basis function network is adopted to determine the optimal process parameters. It is found through the numerical result that the weldline reduction can successfully be achieved. Weldline is generally formed when two or more melt fronts meet, and it is important to vary the flow of melt plastic for the weldline reduction. It is clarified through the numerical result that the local heating can vary the flow of melt plastic that results in the weldline reduction. Based on the numerical result, the experiment using the PIM machine (MS100, Sodick) is conducted. The weldline is well reduced in the experiment, whereas the burn is also observed. It is important to carefully select not only the range of process parameters but also the specification of heater. Through the numerical and experimental result, the validity of the heater-assisted RHCM has been confirmed.

Declarations

Ethical approval This manuscript includes no ethical issues of life science fields.

Consent to participate I have already gotten consent of all authors to participate.

Consent for publication I have already gotten consent of all authors to publish.

Competing interests The authors declare no competing interests.

References

1. Fernandes C, Pontes AJ, Viana JC, Gaspar-cunha A (2018) Modeling and optimization of the injection-molding process: a review. Adv Polym Technol 37:21683. https://doi.org/10.1002/adv.21683

2. Li H, Guo Z, Li D (2007) Reducing the effects of weldlines on appearance of plastic products by Taguchi experimental method. Int J Adv Manuf Technol 32:927–931. https://doi.org/10.1007/s00170-006-0411-z

3. Wu CH, Liang WJ (2005) Effects of geometry and injection-molding parameters on weld-line strength. Polym Eng Sci 45(7):1021–1030. https://doi.org/10.1002/pen.20369

4. Ozcelik B (2011) Optimization of injection parameters for mechanical properties of specimens with weld line of polypropylene using Taguchi method. Int Commun Heat Mass Transfer 38:1067–1072. https://doi.org/10.1016/j.icheatmasstransfer.2011.04.025

5. Kim K, Park JC, Suh YS, Koo BH (2017) Interactive robust optimal design of plastic injection products with minimum weldlines. Int J Adv Manuf Technol 88:1333–1344. https://doi.org/10.1007/s00170-016-8854-3

6. Deng YM, Zheng D, Lu XJ (2008) Injection moulding optimisation of multi-class design variables using a PSO algorithm. Int J Adv Manuf Technol 39:690–698. https://doi.org/10.1007/s00170-007-1258-7

7. Kitayama S, Tamada K, Takano M, Aiba S (2018) Numerical and experimental investigation on process parameters optimization in plastic injection molding for weldlines reduction and clamping force minimization. Int J Adv Manuf Technol 97:2087–2098. https://doi.org/10.1007/s00170-018-2021-y

8. Feng QQ, Zhou X (2019) Automated and robust multi-objective optimal design of thin-walled product injection process based on hybrid RBF-MOGA. Int J Adv Manuf Technol 101:2217–2231. https://doi.org/10.1007/s00170-018-3084-5

9. Zhou H, Zhang S, Wang Z (2021) Multi-objective optimization of process parameters in plastic injection molding using a differential sensitivity fusion method. Int J Adv Manuf Technol 114:423–449. https://doi.org/10.1007/s00170-021-06762-8

10. Yao D, Chen SC, Kim BH (2008) Rapid thermal cycling of injection molds: an overview on technical approaches and applications. Adv Polym Technol 27:233–255. https://doi.org/10.1002/adv.20136

11. Chen SC, Jong WR, Chang JA (2006) Dynamic mold surface temperature control using induction heating and its effects on the surface appearance of weld line. J Appl Polym Sci 101:1174–1180. https://doi.org/10.1002/app.24070

12. Chang PC, Hwang SJ (2006) Experimental investigation of infrared rapid surface heating for injection molding. J Appl Polym Sci 102:3704–3713. https://doi.org/10.1002/app.24515

13. Li X, Zhao GQ, Guan YJ, Ma MX (2009) Optimal design of heating channels for rapid heat cycle injection molding based on response surface and genetic algorithm. Mater Des 30:4317–4323. https://doi.org/10.1016/j.matdes.2009.04.016

14. Zhao G, Wang G, Guan Y, Li H (2011) Research and application of a new rapid heat cycle molding with electric heating and coolant cooling to improve the surface quality of large LCD TV panels. Polym Adv Technol 22:476–487. https://doi.org/10.1002/pat.1536

15. Wang G, Zhao G, Li H, Guan Y (2010) Research of thermal response simulation and mold structure optimization for rapid heat cycle molding processes, respectively, with steam heating and electric heating. Mater Des 31:382–395. https://doi.org/10.1016/j.matdes.2009.06.010

16. Wang G, Zhao G, Li H, Guan Y (2011) Multi-objective optimization design of the heating/cooling channels of the steam-heating rapid thermal response mold using particle swarm optimization. Int J Therm Sci 50:790–802. https://doi.org/10.1016/j.ijthermalsci.2011.01.005

17. Wang G, Zhao G, Guan Y (2011) Research on optimum heating system design for rapid thermal response mold with electric heating based on response surface methodology and particle swarm optimization. J Appl Polym Sci 119:902–921. https://doi.org/10.1002/app.32771

18. Wang G, Zhao G, Guan Y (2013) Thermal response of an electric heating rapid heat cycle molding mold and its effect on surface appearance and tensile strength of the molded part. J Appl Polym Sci 128:1339–1352. https://doi.org/10.1002/app.38274

19. Wang M, Dong J, Wang W, Zhou J, Dai Z, Zhuag X, Yao X (2013) Optimal design of medium channels for water-assisted rapid thermal cycle mold using multi-objective evolutionary algorithm and multi-attribute decision-making method. Int J Adv Manuf Technol 68:2407–2417. https://doi.org/10.1007/s00170-013-4868-2

20. Xiao CL, Huang HX (2014) Multiobjective optimization design of heating system in electric heating rapid thermal cycle mold for yielding high gloss parts, Journal of Applied Polymer Science, 131. https://doi.org/10.1002/app.39976.

21. Xiao CL, Huang HX (2014) Optimal design of heating system for rapid thermal cycle mold using particle swarm optimization and finite element method. Appl Therm Eng 64:462–470. https://doi.org/10.1016/j.applthermaleng.2013.12.062

22. Wang G, Zhao G, Wang X (2014) Heating/cooling channels design for an automotive interior part and its evaluation in rapid heat cycle molding. Mater Des 59:310–322. https://doi.org/10.1016/j.matdes.2014.02.047

23. Wang G, Hui Y, Zhang L, Zhao G (2018) Research on temperature and pressure responses in the rapid mold heating and cooling method based on annular cooling channels and electric heating. Int J Heat Mass Transf 116:1192–1203. https://doi.org/10.1016/j.ijheatmasstransfer.2017.09.126

24. Kitayama S, Ishizuki R, Takano M, Kubo Y, Aiba S (2019) Optimization of mold temperature profile and process parameters for weld line reduction and short cycle time in rapid heat cycle molding. Int J Adv Manuf Technol 103:1735–1744. https://doi.org/10.1007/s00170-019-03685-3

25. Kirchheim A, Katrodiya Y, Zumofen L, Ehrig F, Wick C (2021) Dynamic conformal cooling improves injection molding. Int J Adv Manuf Technol 114:107–116. https://doi.org/10.1007/s00170-021-06794-0

26. Xiao CL, Huang HX (2014) Development of a rapid thermal cycling molding with electric heating and water impingement cooling for injection molding applications. Appl Therm Eng 73:712–722. https://doi.org/10.1016/j.applthermaleng.2014.08.027

27. Xiao CL, Huang HX, Yang X (2016) Development and application of rapid thermal cycle molding with electric heating for improving surface quality of microcellular injection molded parts. Appl Therm Eng 100:478–489. https://doi.org/10.1016/j.applthermaleng.2016.02.045

28. Wang G, Zhao G, Wang X (2013) Effects of cavity surface temperature on mechanical properties of specimens with and without a weld line in rapid heat cycle molding. Mater Des 46:457–472. https://doi.org/10.1016/j.matdes.2012.10.054

29. Wang X, Zhao G, Wang G (2013) Research on the reduction of sink mark and warpage of the molded part in rapid heat cycle molding process. Mater Des 47:779–792. https://doi.org/10.1016/j.matdes.2012.12.047

30. Nian SC, Wu CY, Huang MS (2015) Warpage control of thin-walled injection molding using local mold temperatures. Int Commun Heat Mass Transfer 61:102–110. https://doi.org/10.1016/j.icheatmasstransfer.2014.12.008

31. Shayfull Z, Sharif S, Zain AM, Ghazali MF, Saad RM (2014) Potential of conformal cooling channels in rapid heat cycle molding: a review. Adv Polym Technol 33:21381. https://doi.org/10.1002/adv.21381

32. Kuo CC, Zhu YJ, Wu YZ, You ZY (2019) Development and application of a large injection mold with conformal cooling channels. Int J Adv Manuf Technol 103:689–701. https://doi.org/10.1007/s00170-019-03614-4

33. Kuo CC, Jiang ZF, Lee JH (2019) Effect of cooling time of molded parts on rapid injection molds with different layouts and surface roughness of conformal cooling channels. Int J Adv Manuf Technol 103:2169–2182. https://doi.org/10.1007/s00170-019-03694-2

34. Feng S, Kamat AM, Pei Y (2021) Design and fabrication of conformal cooling channels in molds: review and progress updates,

35. Ozcelik B, Kuram E, Topal MM (2012) Investigation the effects of obstacle geometries and injection molding parameters on weld line strength using experimental and finite element methods in plastic injection molding. Int Commun Heat Mass Transfer 39:275–281. https://doi.org/10.1016/j.icheatmasstransfer.2011.11.012

36. Kitayama S (2022) Process parameters optimization in plastic injection molding using metamodel-based optimization: a comprehensive review. Int J Adv Manuf Technol 121:7117–7145. https://doi.org/10.1007/s00170-022-09858-x

37. Kitayama S, Hashimoto S, Takano M, Yamazaki Y, Kubo Y, Aiba S (2020) Multi-objective optimization for minimizing weldline and cycle time using variable injection velocity and variable pressure profile in plastic injection molding. Int J Adv Manuf Technol 107:3351–3361. https://doi.org/10.1007/s00170-020-05235-8

38. Kitayama S, Arakawa M, Yamazaki K (2011) Sequential approximate optimization using radial basis function network for engineering optimization. Optim Eng 12:535–557. https://doi.org/10.1007/s11081-010-9118-y

39. Kitayama S, Saikyo M, Kawamoto K, Yamamichi K (2015) Multi-objective optimization of blank shape for deep drawing with variable blank holder force via sequential approximate optimization. Struct Multidiscip Optim 52:1001–1012. https://doi.org/10.1007/s00158-015-1293-1

40. Kitayama S, Koyama H, Kawamoto K, Noda T, Yamamichi K, Miyasaka T (2017) Numerical and experimental case study on simultaneous optimization of blank shape and variable blank holder force trajectory in deep drawing. Struct Multidiscip Optim 55:347–359. https://doi.org/10.1007/s00158-016-1484-4

41. Kitayama S, Koyama H, Kawamoto K, Miyasaka T, Yamamichi K, Noda T (2017) Optimization of blank shape and segmented variable blank holder force trajectories in deep drawing using sequential approximate optimization. Int J Adv Manuf Technol 91:1809–1821. https://doi.org/10.1007/s00170-016-9877-5

42. Kitayama S, Kadoya S, Takano M, Kobayashi A (2021) Multi-objective optimization of process parameters in cold forging minimizing risk of crack and forging energy. Arch Civil Mech Eng 21:132. https://doi.org/10.1007/s43452-021-00289-1

43. Kitayama S, Saikyo M, Nishio Y, Tsutsumi K (2015) Torque control strategy and optimization for fuel consumption and emission reduction in parallel hybrid electric vehicles. Struct Multidiscip Optim 52:595–611. https://doi.org/10.1007/s00158-015-1254-8

44. Wu CY, Ku CC, Pai HY (2011) Injection molding optimization with weld line design constraint using distributed multi-population genetic algorithm. Int J Adv Manuf Technol 52:131–141. https://doi.org/10.1007/s00170-010-2719-y

45. Li XP, Zhao GQ, Guan YJ, Ma MX (2010) Multi-objective optimization of heating channels for rapid heat cycle injection mold using Pareto-based genetic algorithm. Polym Adv Technol 21:669–678. https://doi.org/10.1002/pat.1488